

Gravity-driven instability in a spherical Hele-Shaw cell

José A. Miranda, Fernando Parisio, and Fernando Moraes

Laboratório de Física Teórica e Computacional, Departamento de Física, Universidade Federal de Pernambuco, Recife, PE 50670-901 Brazil

Michael Widom

Department of Physics, Carnegie Mellon University, Pittsburgh, Pennsylvania 15213

(Received 7 September 2000; published 27 December 2000)

A pair of concentric spheres separated by a small gap form a spherical Hele-Shaw cell. In this cell an interfacial instability arises when two immiscible fluids flow. We derive the equation of motion for the interface perturbation amplitudes, including both pressure and gravity drivings, using a mode coupling approach. Linear stability analysis shows that mode growth rates depend upon interface perimeter and gravitational force. Mode coupling analysis reveals the formation of fingering structures presenting a tendency toward finger tip-sharpening.

DOI: 10.1103/PhysRevE.63.016311

PACS number(s): 47.20.-k, 68.05.-n, 47.54.+r

I. INTRODUCTION

The Saffman-Taylor instability [1] has been the object of extensive study during the last four decades [2]. It arises at the interface separating two viscous fluids constrained to flow in the narrow gap between closed spaced parallel plates, a device known as Hele-Shaw cell. The cell thickness is smaller than any other length scale in the problem, so the flow is effectively two-dimensional. The instability arises either from a pressure gradient advancing the less viscous fluid against the more viscous one, or by gravity acting on the density difference between the fluids. The action of such driving-force mechanisms leads to the celebrated viscous fingering patterns [1,2].

Most Saffman-Taylor investigations analyze flow between *flat* Hele-Shaw cells. In a separate work [3] we started studying the Saffman-Taylor problem on curved surfaces by considering flow in a *spherical* Hele-Shaw cell (Fig. 1). The interfacial instability was produced by a nonzero flow injection rate Q , and gravitational effects were completely neglected. We examined the effect of cell curvature on the shape of the patterns and showed that positive spatial curvature inhibits finger tip-splitting.

In the present paper we focus on the influence of gravity in a spherical Hele-Shaw cell. We consider both $Q=0$ and $Q>0$ at fixed cell curvature. The unperturbed domain shape is a polar cap of some size, presenting an initially nearly circular boundary, which is gravitationally unstable and evolves at constant area ($Q=0$), or slowly increasing area ($Q>0$), without change of topology.

The study of viscous flow in a nonplanar Hele-Shaw cell is of interest for both scientific and practical reasons. On the scientific level, the influence of spatial curvature on hydrodynamic flow is a matter of fundamental interest. It also provides a simple mathematical model to describe more general situations involving the filling of a thin cavity between two walls of a given shape with fluid. On the practical level, it may have applications in a number of industrial, manufacturing processes, ranging through pressure moulding of molten metals and polymer materials [4], and formation of coat-

ing defects in drying paint thin films [5].

The gravity-driven instability on a spherical Hele-Shaw cell also allows one to gain insight into the properties of the dynamically similar, but more complex, Rayleigh-Taylor instability [6–8] for flow on substrates of arbitrary shapes. One familiar example of this type of instability is the formation of fingering patterns when chocolate syrup drains, due to the action of gravity, from the top of a scoop of ice cream. Despite the apparent simplicity of this example, it is in fact a rather complicated three-dimensional problem [5], much less amenable to analytic treatment than its two-dimensional Hele-Shaw counterpart.

The geometrically constrained spherical Hele-Shaw cell forces the flow to become essentially two-dimensional, and the interface one-dimensional. High viscosity eliminates inertial terms from the equations of motion, making the problem simpler yet. In contrast, the conventional Rayleigh-Taylor problem is inertially driven and three-dimensional effects become important [6–8].

The outline of the work is the following: Sec. II derives the nonlinear equation of motion including both injection and gravitational driving. Section III discusses the resulting motion. Section III A considers linear stability analysis for

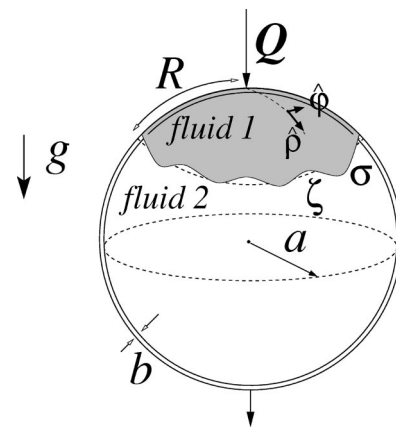


FIG. 1. Schematic configuration of flow in a spherical Hele-Shaw cell.

purely gravitational driving with $Q=0$. The growth is purely exponential, and the linear growth rate depends on the geodesic distance from the sphere's north pole. Larger distance causes both faster growth and more unstable modes, though the characteristic wavelength is nearly constant. The nonvanishing injection case $Q>0$ is studied in Sec. III B. Injection of a high viscosity fluid tends to stabilize the interface. For $Q>0$ linear growth is non-exponential due to evolution of the linear growth rate with distance. Section III C studies the coupling of a small number of modes. It is shown that for gravity-driven flow fingers have tendency to finger tip-sharpening.

II. STABILITY ANALYSIS AND MODE COUPLING

Consider two immiscible, incompressible, viscous fluids, flowing in a spherical Hele-Shaw cell of thickness b (see Fig. 1). The effectively two-dimensional flow takes place on the surface of a sphere endowed with the metric [9]

$$ds^2 = d\rho^2 + a^2 \sin^2\left(\frac{\rho}{a}\right) d\varphi^2, \quad (1)$$

where a is the radius of curvature of the sphere, $0 \leq \varphi < 2\pi$ denotes the azimuthal angle measured on the sphere and $0 \leq \rho \leq \pi a$ is the geodesic distance from the sphere's north pole. The polar angle $\theta = \rho/a$. Denote the viscosities and densities of the upper and lower fluids, respectively, as η_1 , ϱ_1 and η_2 , ϱ_2 . Consider the case $\varrho_1 > \varrho_2$ and $\eta_1 > \eta_2$, and examine flow in the northern hemisphere $\theta < \pi/2$. Between the two fluids there exists a surface tension σ . The flows are assumed to be irrotational, except at the interface. Fluid 1 is injected into fluid 2 through an inlet located at the sphere's north pole, at a given flow rate Q , which is the area covered per unit time. Fluid 2 is simultaneously withdrawn, at the same rate, through an outlet placed at the south pole. The acceleration of gravity is constant, represented by \mathbf{g} , and points from north to south pole.

During the flow, the fluid-fluid interface has a perturbed shape described as $\rho = \mathcal{R} \equiv R(t) + \zeta(\varphi, t)$. The interface perturbation amplitude is represented by $\zeta(\varphi, t)$, and R denotes the time-dependent unperturbed radius

$$R(t) = a \arccos\left(C_0 - \frac{Qt}{2\pi a^2}\right), \quad (2)$$

where $C_0 = \cos(R_0/a)$, and R_0 is the unperturbed radius at $t = 0$. The unperturbed shape is a polar cap of geodesic radius $\rho = R$, surface area $\mathcal{A} = 4\pi a^2 \sin^2(R/2a)$ and circumference $\mathcal{L} = 2\pi a \sin(R/a)$.

We express the net perturbation $\zeta(\varphi, t)$ as a Fourier series

$$\zeta(\varphi, t) = \sum_{n=-\infty}^{+\infty} \zeta_n(t) \exp(in\varphi), \quad (3)$$

where $\zeta_n(t)$ denotes the complex Fourier mode amplitudes, and $n=0, \pm 1, \pm 2, \dots$ is the discrete azimuthal wave number. The area of the perturbed shape is kept independent

of the perturbation ζ by expressing the zeroth Fourier mode in Eq. (3) as $\zeta_0(t) = (-1/2a) \cot(R/a) \sum_{n \neq 0} |\zeta_n(t)|^2$.

We consider a generalized version of Darcy's law [1,2], adjusted to describe flow between concentric spheres

$$\mathbf{v}_j = -\frac{b^2}{12\eta_j} \left[\nabla p_j - \varrho_j g \sin\left(\frac{\rho}{a}\right) \hat{\rho} \right], \quad (4)$$

where $\mathbf{v}_j = \mathbf{v}_j(\rho, \varphi)$ and $p_j = p_j(\rho, \varphi)$ are, respectively, the velocity and pressure in fluids $j=1$ and 2. The gradient in Eq. (4) is associated with the metric (1) and is obtained from the corresponding three-dimensional expression for the gradient in spherical coordinates (r, θ, φ) , by keeping $r=a$ and noting that $\theta = \rho/a$. In contrast to gravity-driven flows in flat Hele-Shaw cells, the gravity term in Eq. (4) is not constant, but depends on the radial distance ρ . This is a manifestation of the cell spatial curvature together with its embedding in three dimensional space.

We can exploit the irrotational flow condition to define the velocity potential $\mathbf{v}_j = -\nabla \phi_j$. Using the velocity potential, we evaluate Eq. (4) for each of the fluids on the interface, subtract the resulting equations from each other, and divide by the sum of the two fluids' viscosities to get

$$A \left(\frac{\phi_1|_{\mathcal{R}} + \phi_2|_{\mathcal{R}}}{2} \right) - \left(\frac{\phi_1|_{\mathcal{R}} - \phi_2|_{\mathcal{R}}}{2} \right) = -\alpha (\kappa)|_{\mathcal{R}} - \gamma a \cos\left(\frac{\mathcal{R}}{a}\right), \quad (5)$$

where $A = (\eta_2 - \eta_1)/(\eta_2 + \eta_1)$ is the viscosity contrast, $\alpha = b^2 \sigma / [12(\eta_1 + \eta_2)]$ contains the surface tension, and $\gamma = b^2 g (\varrho_1 - \varrho_2) / [12(\eta_1 + \eta_2)]$ is a measure of gravitational force. To obtain Eq. (5) we used the pressure boundary condition $p_2 - p_1 = \sigma \kappa$ at the interface $\rho = \mathcal{R}$, where κ is the interfacial curvature [3].

Following steps similar to those performed in Ref. [3], we define Fourier expansions for the velocity potentials, which obey Laplace's equation. We express ϕ_j in terms of the perturbation amplitudes ζ_n by considering the kinematic boundary condition for flow on a sphere. As in the flat cell case, this condition refers to the continuity of the normal velocity across the fluid-fluid interface [10]. Substituting these relations into Eq. (5), and Fourier transforming, yields the mode coupling equation of the Saffman-Taylor problem in a spherical Hele-Shaw cell, taking into account both injection and gravity

$$\dot{\zeta}_n = \lambda(n) \zeta_n + \sum_{n' \neq 0} [F(n, n') \zeta_{n'} \zeta_{-n'} + G(n, n') \zeta_{n'} \zeta_{-n'}], \quad (6)$$

where

$$\lambda(n) = \left[\frac{Q}{2\pi a^2 S^2} (A|n| - C) - \frac{\alpha}{a^3 S^3} |n|(n^2 - 1) + |n| \frac{\gamma}{a} \right] \quad (7)$$

is the linear growth rate, and

$$F(n, n') = \frac{|n|}{aS} \left\{ \frac{QAC}{2\pi a^2 S^2} \left[\frac{1}{2} - \text{sgn}(nn') \right] - \frac{\alpha C}{a^3 S^3} \left[1 - \frac{n'}{2}(3n' + n) \right] + \frac{\gamma C}{2a} \right\} + \frac{Q}{4\pi a^3 S}, \quad (8)$$

$$G(n, n') = \frac{1}{aS} \{ A|n|[1 - \text{sgn}(nn')] - C \} \quad (9)$$

are the second-order mode coupling terms, with $S = \sin(R/a)$ and $C = \cos(R/a)$. The overdot denotes total time derivative and the sign function $\text{sgn}(nn') = 1$ if $(nn') > 0$ and $\text{sgn}(nn') = -1$ if $(nn') < 0$.

III. DISCUSSION

A. Linear stability analysis with $Q=0$

First concentrate on the purely gravity-driven case, $Q=0$. In this situation, we consider flow in a closed cell obeying mass conservation. To drive the interface gravitationally, one could first allow the system to form a stable, unperturbed spherical cap at the south pole, and then invert the spherical cell to put the denser fluid on top in the unstable position at the north pole.

We begin by investigating the dispersion relation (7). Notice that the gravity term in Eq. (7) contains no explicit dependence on radial distance. This finding is somewhat surprising, since the gravity term in Darcy's law (4) clearly presents a dependence on ρ . Physical intuition suggests a factor of S should multiply the gravity term in Eq. (7), making it vanish at the poles and become maximal at the equator. This apparent missing factor reappears if we rewrite the linear growth rate in terms of the wave number $k = |n|/aS$. The variables n and k are both useful: For example, n occurs in integer values and counts the number of fingers. On the other hand, k determines the characteristic wavelength of a perturbation.

To better understand the physical information behind the description of the linear stage in terms of n and k , we plot the linear growth rate at a sequence of radial distances $R = a\theta$ in Figs. 2(a) and 2(b). We use typical experimental parameters given in a recent experimental work in rotating, flat Hele-Shaw cells [11]: fluid 1 is a silicone oil ($\eta_1 \approx 0.5$ g/cm s, $\rho_1 \approx 1.0$ g/cm³) and fluid 2 is air ($\eta_2 \approx 0$, $\rho_2 \approx 0$). The thickness of the cell $b = 0.1$ cm and the surface tension $\sigma = 20.7$ dyne/cm. We set the radius of the sphere $a = 5$ cm and acceleration of gravity $g = 980$ cm/s².

Comparing Figs. 2(a) and 2(b), it is clear that the fastest growing mode (number of fingers n developing at a maximum growth rate) moves to large n for large radial distance (and small n for small radial distance) in order to keep the corresponding fastest growing k , and thus the apparent wavelength, nearly constant. The same effect occurs in radial flow in flat space [12]. In addition to the shift to larger n , the

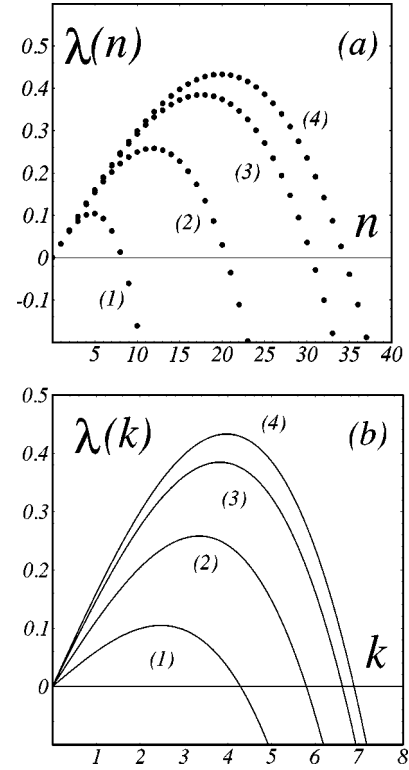


FIG. 2. Linear growth rate as a function of (a) mode number n and (b) wave number k at a sequence of radial distances (1) $R = a\pi/8$, (2) $R = a\pi/4$, (3) $R = a3\pi/8$, and (4) $R = a\pi/2$.

growth rate of the fastest growing mode increases with radial distance because the net gravitational force depends on R . This differs from the case of radial flow in flat space [12], where the interface velocity falls off as $1/R$ causing the growth rate of the fastest growing mode to decrease.

Consider the purely linear contribution, which appears as the first term on the right-hand side of Eq. (6). The condition $Q=0$ simplifies the theoretical description: $R(t) = R_0 = \text{constant}$, and consequently the linear growth rate $\lambda(n)$ is *time independent*. This implies that the actual relaxation or growth of mode n is purely exponential

$$\zeta_n^{(Q=0)}(t) = \zeta_n(0) \exp[\lambda(n)t], \quad (10)$$

where $\zeta_n(0)$ is the initial perturbation amplitude. To see the overall effect of Eq. (10), we plot evolved interfaces using the same experimental parameters as those used in Figs. 2(a) and 2(b). It is convenient to rewrite the net perturbation (3) in terms of cosine and sine modes $\zeta(\theta, t) = \zeta_0 + \sum_{n>0} [a_n(t)\cos(n\theta) + b_n(t)\sin(n\theta)]$, where $a_n = \zeta_n + \zeta_{-n}$ and $b_n = i(\zeta_n - \zeta_{-n})$ are real-valued. We take into account modes n ranging from $n=1$ up to 20. Figure 3 depicts the evolution of the interfaces, for a random choice of phases, at time $t = 5$ s. We evolve from two distinct initial radii (a) $R_0 = a\pi/8$, and (b) $R_0 = a\pi/4$. In both cases $|\zeta_n(0)| = 0.05$ cm and we use the same randomly chosen phases. It is evident that for larger radial distances (or equivalently, larger polar angles) we have both faster growth and more

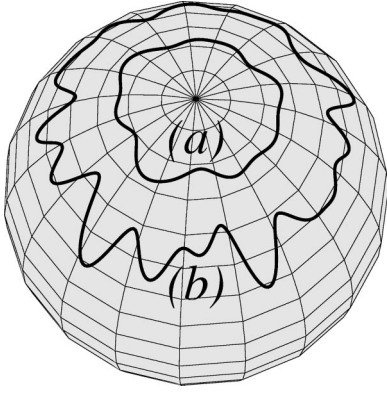


FIG. 3. Interface evolution according to Eq. (10) at $t=5$ s, for (a) $R_0 = a \pi/8$ and (b) $R_0 = a \pi/4$. Other parameters are given in the text.

unstable modes, though the characteristic wavelength is not very different, in agreement with the predictions made from Figs. 2(a) and 2(b).

B. Linear stability analysis with $Q > 0$

Now consider the nonvanishing injection case. Taking $Q > 0$ introduces two important new effects. First, inspecting Eq. (7), we see that Q multiplies a term linear in n that must be added to the growth rate λ obtained with $Q=0$. If the inner fluid is high viscosity, so that $A < 0$, then this new term in λ is negative. All modes grow more slowly with $Q > 0$, and some may even become stable. Thus, $Q > 0$ diminishes the strength of the instability. Essentially, the flow fills in the gaps between the fingers.

The second effect is more subtle. Since the unperturbed interface radius $R(t)$ is now *time dependent*, the linear growth rate λ evolves with time as the radial distance steadily grows. At any instant the interface evolves exponentially with an instantaneous growth rate λ depending on the current $R(t)$. For sufficiently small Q the instantaneous λ at $R(t)$ nearly equals the $Q=0$ value for the same $R(t)$. We call this a *quasistatic* approximation, and within this approximation it is clear that an increasing number of modes become unstable as time progresses due to the steady increase of $R(t)$. The evolution of λ in the quasistatic approximation is given by the series of curves shown in Fig. 2.

If we wish to study the linear growth *without* making the quasistatic approximation, we may integrate the equation of motion (6) exactly, keeping only terms of first order in ζ on the right-hand side. Because λ is time dependent, through the variation of $R(t)$, the exact solution of the linear equation of motion becomes non-exponential and can be written as

$$\begin{aligned} \zeta_n^{(Q>0)}(t) = & \zeta_n(0) \frac{S_0}{S} \left[\frac{\tan(R/2a)}{\tan(R_0/2a)} \right]^{A|n|} \\ & \times \exp \left\{ \frac{2\pi|n|}{Q} \left[\frac{\alpha(n^2-1)}{a} \left(\frac{C}{S} - \frac{C_0}{S_0} \right) \right. \right. \\ & \left. \left. + \gamma a(C_0 - C) \right] \right\}, \end{aligned} \quad (11)$$

where $S_0 = \sin(R_0/a)$, and R , C , and S all depend on time.

C. Mode coupling analysis

We use the mode coupling equation (6) to investigate the effect of the nonlinear terms in the interface evolution. We are interested in studying how gravity influences the shape of the fingering structures, focusing on finger-tip behavior. Finger-tip splitting and tip-sharpening phenomena are related to the influence of a fundamental mode n on the growth of its harmonic $2n$. Without loss of generality we may choose the phase of the fundamental mode so that $a_n > 0$ and $b_n = 0$. We replace the time derivative terms \dot{a}_n and \dot{b}_n by $\lambda(n) a_n$ and $\lambda(n) b_n$, respectively, for consistent second order expressions. Under these circumstances the equation of motion for the harmonic cosine mode becomes

$$\dot{a}_{2n} = \lambda(2n) a_{2n} + \frac{1}{2} T(2n, n) a_n^2 \quad (12)$$

where the finger-tip function is

$$\begin{aligned} T(2n, n) = & \frac{2n}{aS} \left\{ \frac{Q}{2\pi a^2 S^2} \left[\frac{(C^2+1)}{4n} - AC \right] \right. \\ & \left. + \frac{3\alpha C(2n^2-1)}{2a^3 S^3} \right\}. \end{aligned} \quad (13)$$

The corresponding equation for the sine modes b_{2n} is not as interesting as Eq. (12), since growth of b_{2n} is uninfluenced by a_n .

The sign of $T(2n, n)$ dictates whether finger-tip splitting or finger tip-sharpening is favored by the dynamics [12]. If $T(2n, n) < 0$, at second order the result is a driving term of order a_n^2 forcing growth of $a_{2n} < 0$. With this particular phase of the harmonic forced by the dynamics, the n outwards-pointing fingers of the fundamental mode n tend to split. In contrast, if $T(2n, n) > 0$ growth of $a_{2n} > 0$ would be favored, leading to outwards-pointing finger-tip sharpening.

A noteworthy point about Eq. (13) is that it shows no dependence whatsoever on gravity. In the evaluation of $T(2n, n)$ from Eq. (6) we found that the term involving gravity in $F(2n, n)$ exactly cancels against the term involving gravity in $\lambda(n)G(2n, n)$. The second order term driving tip-splitting in Eq. (12) is therefore independent of the force of gravity, though gravity does generally influence mode coupling at second and higher orders.

Inspecting Eq. (13) we find that, since $A = -1$ and $C > 0$, the finger-tip function $T(2n, n) > 0$ for both $Q=0$ and $Q > 0$. Equation (13) predicts that gravity-driven flow on a sphere leads to patterns showing enhanced finger-tip narrowing. Informal studies of chocolate syrup fingers on ice cream scoops support this claim.

ACKNOWLEDGMENTS

J.A.M., F.P., and F.M. thank CNPq and FINEP for financial support. Work of M.W. was supported in part by the National Science Foundation Grant No. DMR-9732567.

- [1] P. G. Saffman and G. I. Taylor, Proc. R. Soc. London, Ser. A **245**, 312 (1958).
- [2] D. Bensimon, L. P. Kadanoff, S. Liang, B. I. Shraiman, and C. Tang, Rev. Mod. Phys. **58**, 977 (1986); G. Homay, Annu. Rev. Fluid Mech. **19**, 271 (1987); K. V. McCloud and J. V. Maher, Phys. Rep. **260**, 139 (1995).
- [3] F. Parisio, F. Moraes, J. A. Miranda, and M. Widom, submitted to Phys. Rev. E (2000).
- [4] S. Richardson, J. Fluid Mech. **56**, 609 (1972).
- [5] L. W. Schwartz and D. E. Weidner, J. Eng. Math. **29**, 91 (1995).
- [6] Lord Rayleigh, *Scientific Papers, Vol. II* (Cambridge University Press, Cambridge, England, 1900).
- [7] G. I. Taylor, Proc. R. Soc. London, Ser. A **201**, 192 (1950).
- [8] S. Chandrasekhar, *Hydrodynamic and Hydromagnetic Stability* (Oxford University Press, Oxford, 1961).
- [9] B. A. Dubrovin, A. T. Fomenko, and S. P. Novikov, *Modern Geometry-Methods and Applications, Parts 1 and 2* (Springer-Verlag, New York, 1984).
- [10] R. E. Rosensweig, *Ferrohydrodynamics* (Cambridge University Press, Cambridge, England, 1985).
- [11] Ll. Carrillo, J. Soriano, and J. Ortín, Phys. Fluids **12**, 1686 (2000).
- [12] J. A. Miranda and M. Widom, Physica D **120**, 315 (1998).